






ARTICLE

A model-based framework for parallel scale-down fed-batch cultivations in mini-bioreactors for accelerated phenotyping

Emmanuel Anane¹  | Ángel Córcoles García² | Benjamin Haby¹  | Sebastian Hans¹  |
Niels Krausch¹  | Manuel Krewinkel² | Peter Hauptmann² | Peter Neubauer¹ |
Mariano Nicolas Cruz Bournazou^{1,3,4} 

¹Department of Bioprocess Engineering, Institute of Biotechnology, Technische Universität Berlin, Berlin, Germany

²Biologics Development: Microbial Dev't, Sanofi-Aventis Deutschland GmbH, Frankfurt, Germany

³Department of Chemistry and Applied Biosciences, ETH Zurich-Institute of Chemical and Bioengineering, Zurich, Switzerland

⁴DataHow AG, Zurich, Switzerland

Correspondence

Mariano Nicolas Cruz Bournazou, Department of Bioprocess Engineering, Institute of Biotechnology, Technische Universität Berlin, Ackerstraße 76, ACK24, 13355 Berlin, Germany.
Email: nicolas.cruz@ethz.ch

Funding information

H2020 Marie Skłodowska-Curie Actions, Grant/Award Number: 643056

Abstract

Concentration gradients that occur in large industrial-scale bioreactors due to mass transfer limitations have significant effects on process efficiency. Hence, it is desirable to investigate the response of strains to such heterogeneities to reduce the risk of failure during process scale-up. Although there are various scale-down techniques to study these effects, scale-down strategies are rarely applied in the early developmental phases of a bioprocess, as they have not yet been implemented on small-scale parallel cultivation devices.

In this study, we combine mechanistic growth models with a parallel mini-bioreactor system to create a high-throughput platform for studying the response of *Escherichia coli* strains to concentration gradients. As a scaled-down approach, a model-based glucose pulse feeding scheme is applied and compared with a continuous feed profile to study the influence of glucose and dissolved oxygen gradients on both cell physiology and incorporation of noncanonical amino acids into recombinant proinsulin. The results show a significant increase in the incorporation of the noncanonical amino acid norvaline in the soluble intracellular extract and in the recombinant product in cultures with glucose/oxygen oscillations. Interestingly, the amount of norvaline depends on the pulse frequency and is negligible with continuous feeding, confirming observations from large-scale cultivations. Most importantly, the results also show that a larger number of the model parameters are significantly affected by the scale-down scheme, compared with the reference cultivations.

In this example, it was possible to describe the effects of oscillations in a single parallel experiment. The platform offers the opportunity to combine strain screening with scale-down studies to select the most robust strains for bioprocess scale-up.

KEYWORDS

Escherichia coli, mini-bioreactors, modeling, scale-down, scale-up effects

1 | INTRODUCTION

Scale-down bioreactors have been applied in bioprocess development to study the response of microbial cell factories and other expression systems to various stress-inducing concentration gradients (scale-up effects) that occur in large-scale bioreactors (Neubauer & Junne, 2016; Nienow et al., 2013). In the past three decades, both multi-compartment and pulse-based scale-down bioreactor systems have been developed to mimic gradients in large-scale bioreactors, in an attempt to better understand and characterize microbial behavior at an industrial production scale. For instance, a two-compartment scale-down bioreactor with a total volume of 7 L was applied to study the loss in product yield and accumulation of undesirable metabolites in a 12,000 L industrial-scale cultivation of *Escherichia coli* producing human growth hormone (Bylund, Castan, Mikkola, Veide, & Larsson, 2000). The successful operation of a scale-down bioreactor to study a particular process depends on how accurately the scale-down bioreactor mimics the environmental heterogeneity existing in the large-scale bioreactor. Although multi-compartment scale-down bioreactors can provide comprehensive information on cellular responses (Neubauer & Junne, 2010; Neubauer & Junne, 2016), they are complex to operate and not easy to parallelize for early screening approaches.

The widespread use of parallel mini-bioreactor systems for strain screening has been adopted in many bioprocess development settings to help reduce product life cycles and accelerate R&D (Tajsoleiman, Mears, Krühne, Gernaey, & Cornelissen, 2019). The parallelization and automation of such cultivation platforms enable screening of large libraries within shorter times (Back, Rossignol, Krier, Nicaud, & Dhulster, 2016). An initial challenge of these systems was the difficulty in implementation of controlled feeding strategies, as in laboratory bioreactors. However, various solutions have been developed recently to enable fed-batch-like conditions, such as the gradual supply of glucose to the culture through enzyme-based glucose release systems (Krause, Neubauer, & Neubauer, 2016), the application of micro-pumps for continuous feed supply (Gebhardt, Hortsch, Kaufmann, Arnold, & Weuster-Botz, 2011), model-based intermittent feeding (Sawatzki et al., 2018), and membrane-based substrate release systems (Philip et al., 2018). These improvements bring the screening system closer to actual cultivation conditions, such that a better performing strain can be selected for scale-up. However, it is important to note that under normal fed-batch-like screening conditions, the cells still grow in a homogeneous, perfectly mixed environment without perturbations, which may be quite different from actual industrial-scale cultivation conditions. Therefore, the strains selected in these high-throughput platforms for scale-up may not be robust enough at industrial scale. High-throughput experimental facilities that perform fed-batch experiments with frequent glucose perturbations have been reported (Barz, Sommer, Wilms, Neubauer, & Cruz Bournazou, 2018; Cruz Bournazou et al., 2017; Vester, Hans, Hohmann, & Weuster-Botz, 2009).

Nevertheless, the objective of glucose perturbations in these works was to increase process dynamics information in optimal experimental design, and no reference to bioreactor heterogeneities or scale-down efforts was made.

A few studies that consider the operating conditions of larger-scale bioreactors in high-throughput screening systems are reported in the literature. For instance, Janakiraman, Kwiatkowski, Kshirsagar, Ryll, and Huang (2015) matched the volumetric aeration rates (vvm) between parallel *ambr15*TM cultivations of CHO cells and a 15,000-L production-scale bioreactor, whereas Velez-Suberbie et al. (2018) used the power per unit volume (P/V) as a scale-down criterion to compare *ambr15f* cultivations of *E. coli* with 20-L bioreactor cultivations. Other works involving high-throughput cultivations in complex integrated facilities have also been reported (see recent review in Hemmerich, Noack, Wiechert, & Oldiges, 2018). However, although these works point to the right direction in terms of high-throughput bioprocess development, matching only one engineering criterion between scales is not necessarily the same as replicating specific environmental heterogeneities in smaller bioreactors for scale-down studies. The engineering criteria are global parameters of the whole system, whereas scale-up effects arise from zone-specific heterogeneities within industrial bioreactors (Enfors et al., 2001). These heterogeneous environments have specific space-time dynamics in relation to the physiology of the organism. These dynamics must be reproduced on a smaller scale for proper scale-down studies. Unfortunately, the smaller volumes of mini-bioreactor systems pose difficulty in running such representative gradient-based scale-down cultivations in high-throughput systems (Tajsoleiman et al., 2019).

The aim of this study was to apply a high-throughput parallel mini-bioreactor system as a scale-down bioreactor together with a model-based approach to test and evaluate the performance of a possible production strain under oscillating conditions relevant on a large industrial scale. A platform of 21 parallel mini-bioreactors was used, that was coupled to a robotic liquid handling station (LHS) for automated operation of the cultivations. The operation of the LHS was based on mechanistic model outputs which describe both the dynamic physiological behavior of the strain (Anane, López C, Neubauer, & Cruz Bournazou, 2017) and gradient profiles of scale-down bioreactors determined from typical mixing times of large-scale bioreactors (Anane, Sawatzki, Neubauer, & Cruz-Bournazou, 2019). As a demonstration, the platform was used to study the effects of the oscillating glucose/dissolved oxygen concentrations on the amount and quality of recombinant proinsulin expressed in *E. coli* as inclusion bodies. The quality of the protein was assessed by the amount of incorporation of noncanonical branched-chain amino acids (ncBCAA) into the recombinant product. The intracellular synthesis and incorporation of the ncBCAAs norvaline, norleucine, and β -methyl-norleucine was previously described to occur as a result of conditions where oxygen depletion is connected with high glucose concentrations, which can appear in feeding zones of large-scale industrial bioreactors (for a recent review, see Reitz, Fan, & Neubauer, 2018).

Such a high-throughput scale-down system is suitable for the generation of large physiological data under real oscillating conditions/gradients in the early screening phase, which can be used for the validation of metabolic network models that may be applied in scale-up studies (Haringa et al., 2018). In addition, the platform also offers the possibility to compare the response of different candidate strains to concentration gradients during screening and to select the best phenotype for scale-up.

2 | MATERIALS AND METHODS

2.1 | Strain, cultivation conditions, and mini-bioreactor configuration

The scale-down experiments in mini-bioreactors were carried out with *E. coli* BW25113 (*lacI⁺*) pSW3 (*amp^r*; for full genotypic description, see here Grenier, Matteau, Baby, & Rodrigue, 2014), expressing recombinant proinsulin under the isopropyl- β -D-thiogalactopyranosid (IPTG)-inducible *tac*-promoter (provided by Sanofi-Aventis Deutschland GmbH). To make the starting culture, 20 ml of mineral salt medium, supplemented with trace elements (Anane, Sawatzki et al., 2019), 5 g·L⁻¹ glucose and 100 mg·L⁻¹ ampicillin was inoculated with 100 μ l of cryo stock culture in a 125 ml Erlenmeyer flask and incubated at 37°C, 200 rpm in an orbital shaker (Adolf Kühner AG, Birsfelden, Switzerland). The single-use baffled flask was equipped with optical sensor spots for online monitoring of pH and dissolved oxygen tension on the PreSens platform (PreSens-Precision Sensing GmbH, Regensburg, Germany). The pH was controlled by intermittent titration with 7.5% NH₄OH using a routine that was included in the worklist of the LHS robots. After 10 hr of cultivation, whilst in the exponential growth phase, an appropriate volume of the preculture was used to inoculate the bioreactor medium to a final optical density (OD₆₀₀) of 0.1. Then, 10 ml of the inoculated medium was transferred into each mini-bioreactor, under aseptic conditions to start the batch phase of the cultivation. The bioreactor medium consisted of mineral salt medium and trace elements (same as in the preculture), 5 g·L⁻¹ glucose and 30 g·L⁻¹ of EnPump200[®] glucose polymer (Enpresso GmbH, Berlin, Germany). During cultivation, the pH was maintained at a set point of 7.0 by a PI controller with the addition of 6% NH₄OH, and the temperature was maintained at 37°C. The cultivations were done in 15 ml disposable mini-bioreactor vessels (bioREACTOR[®] 48 system; 2mag AG, München, Germany) equipped with a magnetically driven impeller and photo-optical sensor spots for pH and DOT measurement. The bioreactor was connected to a Tecan[®] pipetting robot (Tecan Group Ltd, Männedorf, Switzerland) and to a central database where all online and at-line data were directly saved. The aeration of each mini-bioreactor was achieved by an induced draft mechanism, where the air was drawn into the broth through a hollow shaft on which the impeller was mounted (Puskeiler, Kaufmann, & Weuster-Botz, 2005). By this mechanism, the whole bioreactor block was aerated to 10 L_{air}·min⁻¹ during cultivation. The detailed configuration of hardware-software protocols, sampling algorithms, pH control routines, pulse feed scheduling and off-line, at-line and online analytics

on the robot station during parallel cultivations were presented previously (Cruz Bournazou et al., 2017; Nickel, Cruz-Bournazou, Wilms, Neubauer, & Knepper, 2017; Sawatzki et al., 2018).

2.2 | Calculation of gradient profiles

In aerobic fed-batch cultivations in large industrial-scale bioreactors, zones of higher glucose concentrations (feed zones) are invariably associated with depletion of dissolved oxygen, whereas zones with low glucose concentrations have higher dissolved oxygen concentrations. Thus, both glucose and dissolved oxygen gradients occur simultaneously, although inversely, in larger bioreactors. To mimic such effects in the mini-bioreactors, a mechanistic solution of the pulse-based scale-down concept was developed (Anane, Sawatzki et al., 2019). The pulse frequencies and amplitudes (set point of growth rate μ) were calculated based on the previous simulation of gradient profiles in large-scale bioreactors (Anane, Sawatzki et al., 2019). At the end of the batch phase, both online and at-line data were read directly from the central database of the cultivation platform into a programming environment to ascertain the current state of the cultures. On the basis of the measured data, model-based predictions of biomass and the glucose requirements were calculated; these were then used to define the feeding scheme of the respective cultivation. The mechanistic model of *E. coli* was solved in discrete intervals to obtain glucose concentrations that are equivalent to concentrations experienced by a cell in a large-scale bioreactor at the given mixing times. The pulsing scheme was determined by two timespans: t_{sp} and t_{swof} , which are, respectively, the times of glucose excess and glucose limitation, the sum of which reflects the pulse cycle. The 5 min pulse cycle results in approximate gradient profiles equivalent to those in larger bioreactors with approximately 40 s mixing time, whereas the 10 min pulse cycle is equivalent to 90 s mixing time in actual large-scale bioreactors (Anane, Sawatzki et al., 2019). For each pulse cycle ($t_{se} = t_{sp} + t_{swof}$), the exponential feed profile was integrated to find the volume of feed to be added to obtain a glucose excess (ca. 0.4–0.8 g·L⁻¹) within the period t_{sp} . This was followed by the resting (starvation phase) when glucose was depleted from the medium. The details of the calculations and the actual code are given in a downloadable Matlab file in the Supporting Information Material.

2.3 | Scale-down cultivations in mini-bioreactors

A total of seven cultivation conditions were implemented in triplicates (three parallel mini-bioreactors for each condition) as follows (Table 1):

- i. B1–B3: These were the reference or control cultivations. With 30 g·L⁻¹ of EnPump[®] polymer (Enpresso GmbH) in the medium already, these mini-bioreactors were fed with glucoamylase (also

TABLE 1 Cultivation conditions in 21 parallel mini-bioreactors

Bioreactors	Pulse freq. (min)	IPTG (mM)	Enzyme-based feeding
B1 B2 B3	-	0.5	linearly to 13 U/L
C1 C2 C3	5	0.5	-
D1 D2 D3	5	1.0	-
E1 E2 E3	5	0.5	once, 3 U/L
F1 F2 F3	10	0.5	-
G1 G2 G3	10	1.0	-
H1 H2 H3	10	0.5	once, 3 U/L

Abbreviation: IPTG, isopropyl- β -D-thiogalactopyranosid.

from EnPresso GmbH), in distinct additions every 5 min to a final concentration of 13 U·L⁻¹ at the end of the exponential feeding phase, providing an estimated glucose release rate of 0.85 g·L⁻¹·hr⁻¹ at this enzyme concentration (Mayer et al., 2014). The EnPump polymer is a polysaccharide that is gradually degraded by the added enzyme to release glucose into the medium, such that the cells utilize only the released glucose for growth and not the polymer (Krause et al., 2010). The linear enzyme feed resulted in an approximately exponential glucose release, which then switched to a near-constant release rate when enzyme feeding was stopped (Panula-Perälä et al., 2008).

- ii. C1–C3: These were fed with a glucose pulse every 5 min during the fed-batch phase to mimic concentration gradients experienced in a larger bioreactor with a mixing time of approximately 40 s (Anane, Sawatzki et al., 2019). In the first 3 hr of feeding, the pulse size was increased exponentially to maintain a specific growth rate of 0.35 hr⁻¹ in this phase, after which the pulse size was kept constant, upon IPTG induction. They were induced to a final concentration of 0.5 mM IPTG.
- iii. D1–D3: These had the same feeding condition as C1–C3, but were induced to a final concentration of 1.0 mM IPTG.
- iv. E1–E3: Glucose pulse feed and induction conditions in these bioreactors were the same as those in C1–C3. However, a single dose of amylase (3 U·L⁻¹) was added to this set of bioreactors to ensure a continuous supply of limiting glucose in the background, in addition to the 5-min glucose pulses. The residual glucose supply was calculated to be less than 10% of the glucose requirements to maintain the specific growth rate at the set value. This was to ensure that the culture in these bioreactors does not fall into acute starvation conditions between the pulses.
- v. The last set of nine mini-bioreactors was similar to the previous set of nine, with the only exception that the glucose pulses were administered every 10 min, producing approximate glucose and dissolved oxygen gradients experienced in bioreactors with mixing times of approximately 90 s (Anane, Sawatzki et al., 2019). Thus, C1–C3 \approx F1–F3, D1–D3 \approx G1–G3 and E1–E3 \approx H1–H3, with the exception of a glucose pulse frequency of 10 min in the latter sets, as shown in Table 1.

2.4 | Analyses

For analyses, 300 μ l sample of culture broth was taken from each mini-bioreactor at the end of the batch phase, and thereafter on an hourly basis in the fed-batch phase. Cell growth was monitored by OD at 600 nm. Therefore, 10 μ l of each sample was diluted by a factor of 20 with saline water (0.9% NaCl) in a microwell plate, and the absorbance was measured in a plate reader (Synergy™ MX microwell plate reader; BioTek Instruments GmbH, Bad, Germany). The OD₆₀₀ values were corrected against a blank (0.9% NaCl) and divided by a factor of 0.5 for path length correction to a 1-cm cuvette, as described previously (Cruz Bournazou et al., 2017). The OD₆₀₀ values were converted to dry cell weight using a conversion factor of 0.37 g·L⁻¹ dry weight per 1 OD₆₀₀, which was previously determined for this strain using the same spectrophotometer, with the method described by Glazyrina et al. (2010). The rest of the samples were centrifuged at 15,000g for 5 min, and the supernatant and pellets were separated and stored at -20°C for further analysis.

The concentrations of glucose, acetate, and formate were measured enzymatically on the Cedex Bio HT Analyzer (Roche Diagnostics Int Ltd) with automatic dilution for samples where the calculated analyte concentration was outside the range of concentrations within the calibration curve. A maximum of 10 μ l of thawed supernatant from the samples was required for the enzymatic analysis of the metabolites.

Protein quantification was done by analyzing the cultivation samples and protein standards on a Labchip® GX II Touch (PerkinElmer, Waltham, MA). The cell pellets were re-suspended in 500 μ l phosphate-buffered saline (PBS) and normalized to OD₆₀₀ = 5 in 1 ml. After centrifugation, the pellet from the normalized samples was lysed using Bugbuster® reagent, according to a previously described procedure (Anane, Sawatzki et al., 2019). Further inclusion body purification was carried out using the Bugbuster protocol, also as described previously (Anane, Sawatzki et al., 2019). From this procedure, three sample fractions were isolated for further processing: the raw cell lysate, intracellular soluble fraction, and purified inclusion bodies. For protein quantification, 2 μ l of the raw cell lysate fraction was added to 7 μ l of denaturing solution (700 μ l PBS, 24.5 μ l of 1 M dithiothreitol) in PCR plates. The plate was incubated in a thermal cycler at 100°C for 5 min. After cooling for 5 min at room temperature, the plate was loaded into the Labchip device to run the microchip capillary electrophoresis. Protein quantification was done by running the cultivation samples together with protein standards of similar size (10 kDa) as the recombinant proinsulin (11 kDa). Data analysis (calibration with standards, imaging and quantification) was done using the Labchip Reviewer® software (PerkinElmer). To quantify the concentration of noncanonical amino acids in each sample, both the purified inclusion body and the intracellular soluble fractions were hydrolyzed in concentrated (6 M) HCl, followed by derivatization and analysis of derivatized amino acids on an Agilent GC-MS

system (Agilent Technologies, Waldbronn, Germany) according to the procedure described previously (Anane, Sawatzki et al., 2019). To measure the level of incorporation of ncBCAAs for each cultivation condition, the ratio of the concentrations of the noncanonical form to the respective canonical form of the amino acid in the product was calculated (e.g., moles of norvaline per mole of leucine), given that all samples were normalized to the same biomass concentration before analysis.

3 | RESULTS

3.1 | Growth profiles of *E. coli* in response to glucose and oxygen pulses

To investigate the influence of scale-up effects on the performance of fed-batch processes in a high-throughput platform, *E. coli* BW25113 pSW3 was cultivated under seven different growth conditions. The conditions include glucose and dissolved oxygen gradients, different induction strengths, exposure to intermittent acute starvation zones, and repetitive exposure to overflow conditions. The average of triplicate runs (biological replicates) for each condition is reported in the following sections, except for the concentration of noncanonical amino acids where the average of triplicate measurements (technical replicates) is reported. As there were no differences in set-up among the parallel runs in the batch phase of the cultivation, the discussion is limited to the fed-batch phase of the cultivation. With the same concentration of glucose in the batch phase, all 21 parallel cultivations reached the same average biomass of $2.3 \pm 0.08 \text{ g} \cdot \text{L}^{-1}$ at the end of this phase. The full

results of the various cultivation conditions are shown in Figure SA.1 in Supporting Information Material.

3.1.1 | Effect of pulse frequency in the fed-batch phase

The pulse frequencies of 5 and 10 min led to lower biomass concentrations in the scale-down cultivations in comparison to the continuous reference cultivation, as shown in Figure 1a. The mini-bioreactors that were subjected to 5 and 10 min glucose pulses, respectively, reached 17% and 11% less final biomass concentrations than the reference cultivation. Although the same mass of glucose was fed in both of the pulse-based cultivations, the 10 min pulse frequencies led to approximately 7% higher biomass than the 5 min frequency pulses (Figure 1a).

Despite the relatively lower biomass, the highest concentration of overflow metabolites was measured in the pulse-based cultivations. The final acetate concentration in the 5 min pulse cultivation was approximately fivefold higher than that in the 10 min pulse cultivations, whereas the reference cultivation had virtually no acetate accumulation in the fed-batch phase (Figure 1b). In the 10 min pulse cultivations, a higher concentration of formate was recorded than in the 5 min pulses, but the formate was rapidly consumed when the feed was switched to constant feed (Figure 1c). The frequency of the pulses also influenced the accumulation of inclusion bodies (product) during the cultivations. The 5 min pulse cultivations had 16% and 22% lower final concentration of inclusion bodies per gram of biomass (dry weight basis) than the 10 min pulse and reference cultivations, respectively (Figure 1d).

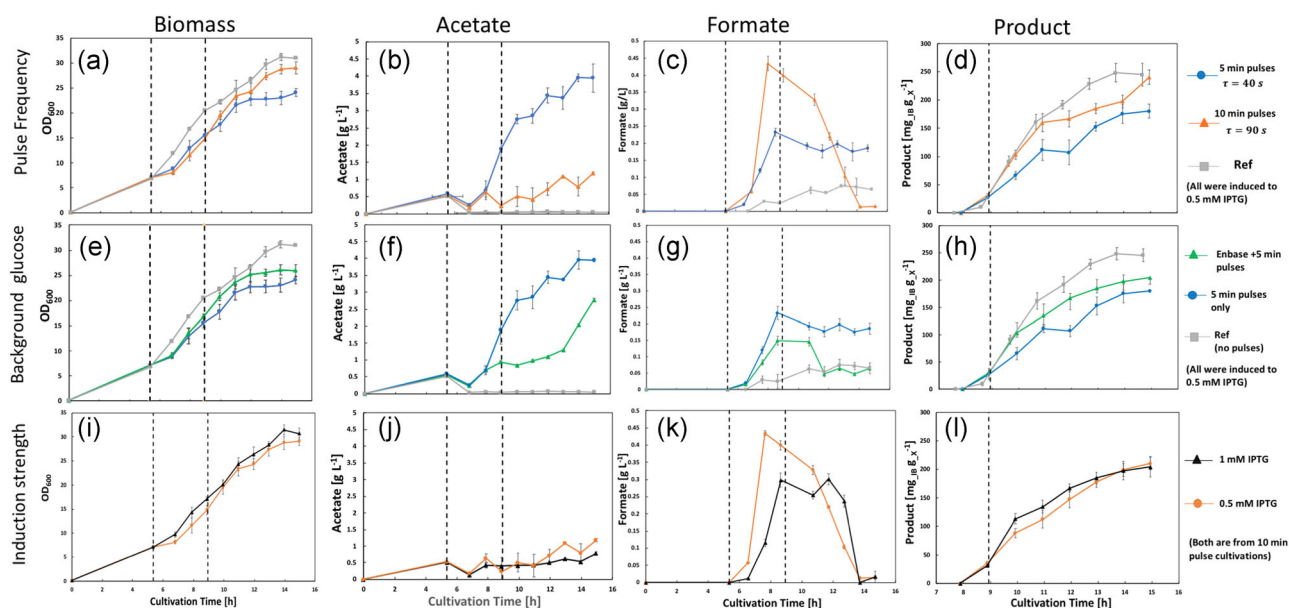


FIGURE 1 Growth profiles of fed-batch cultures of *E. coli* BW25113 pSW3 and metabolite concentrations from 21 parallel cultivations. The detailed conditions are shown in Table 1 and in Materials and Methods. The cultivations have been grouped according to variation in pulse frequency (a–d), presence or absence of an enzymatic glucose supply in the background (e–h) and the strength of IPTG induction (i–l). Profiles of 5 min pulse frequencies in a–d are repeated in e–h. Error bars represent the standard deviation of triplicate cultivations. IPTG, isopropyl- β -D-thiogalactopyranosid [Color figure can be viewed at wileyonlinelibrary.com]

3.1.2 | Effect of background/residual glucose supply

The supply of background glucose through the enzymatic glucose release system led to higher biomass than the corresponding cultivations without background glucose. The 5 min pulse frequency with background glucose led to approximately 7% higher biomass than the same cultivation without glucose release (Figure 1e), whereas the 10 min frequency only recorded 4% higher biomass with the background glucose release. However, this marginal increase in biomass may be due to the 3% higher total glucose fed in these cultivations, which is the contribution of the background glucose from the enzymatic system.

However, contrary to expectations, the residual glucose supply led to lower extracellular metabolite concentrations. For example, in the 5 min pulse frequency cultivations, there was 34% less acetate in the runs with background glucose compared with the pure pulses without background glucose (Figure 1f). The same trends were also recorded for formate profiles, where both the 5 (Figure 1g) and 10 min frequencies accumulated lower concentrations of formate compared with the corresponding cultivations without background glucose.

The accumulation of proinsulin was also slightly influenced by the background glucose supply, with the 5 min frequency (Figure 1h). The final amount of inclusion bodies in the cultivations with background feeding was approximately 6% higher compared with the corresponding cultivations without background glucose feeding. The recombinant product in the reference cultivation was still higher than that in the pulse-based cultivations with the background enzymatic glucose release system.

3.1.3 | Effect of induction strength

As observed in earlier studies (Anane, Sawatzki et al., 2019), the intermittent starvation of *E. coli* cells due to the pulse feeding mechanism partially derepresses the *tac*-promoter, under which the recombinant protein is produced. Therefore, before induction, some amount of inclusion bodies already accumulated in both the 5 and 10 min frequency cultivations (Figures 1d, 1h, and 1l). This preinduction product formation was not observed in the reference cultivation (sample taken immediately before induction) where glucose supply was smooth and continuous. A slightly higher induction strength (1 mM IPTG) did not have any observable influence on cell growth and extracellular metabolite accumulation for the cultivations with 5 and 10 min pulses, respectively (Figure 1i–k). However, the rate of product accumulation was predictably influenced by IPTG concentration. The higher IPTG concentration (1 mM) led to a slightly higher rate of accumulation of inclusion bodies, but this also resulted in a slightly faster saturation of the recombinant protein production rate compared with the cultures which were induced by 0.5 mM IPTG. Apart from the product formation kinetics, which was different between the two IPTG concentrations, the final inclusion body concentration was the same for both (Figure 1l).

3.2 | Model fitting of scale-down cultivations

To further investigate the influence of glucose and dissolved oxygen pulses (gradients) on the metabolic behavior of *E. coli* BW25113, the mechanistic model (see the Supporting Information Material for model description) was fitted to datasets from the scale-down cultivations to estimate the values of parameters that were achieved during the cultivations. The criterion of the model fitting was the minimization of the sum of squares of residuals between the measured data and model predictions, using the interior-point algorithm, which was executed within the global optimization framework GlobalSearch in Matlab® 2016b. As described previously (Anane et al., 2017), the use of structured mechanistic models to describe the physiological states of the culture also allows us to estimate some metabolic states of the culture that are otherwise difficult to measure. The results of the model fitting are shown in Figure 2, whereas parameters that describe maximum specific uptake rates, yield coefficients, and maintain energy levels are compared in Table 2 for the 5 min pulse, 10 min pulse, and reference cultivations. Also, the original parameter values that were used to calculate the feed profiles in the pulse-based fed-batch culture are provided in Table 2.

3.3 | Metabolic responses of *E. coli* to glucose pulses based on model fitting

The parameters in Table 2 were estimated for the overall duration of the cultivation by collating data points from the triplicate runs of each condition. However, to track the time-course evolution of the metabolic fluxes, the estimated parameters and experimental data were used to calculate the specific rates during the cultivation using Equations (A.1)–(A.9) (Appendix). The results are shown in Figure 3. Whereas Table 2 depicts the metabolic potential or the capacity of the strain under each cultivation condition, Figure 3 depicts the actual metabolic states achieved during cultivation under each of the conditions.

The metabolic profiles show lower glucose uptake rates in the reference cultivation, with a lower overflow flux than in the pulse-based cultivations (Figure 3a–c). Noting that the sum of the overflow and oxidative fluxes for each condition is equal to the total glucose uptake rate for that condition, it is apparent that more carbon source was wasted through overflow metabolites in the pulse-based cultivations. This is evident from the ratios of the average overflow flux to the average glucose uptake rate (q_{sof}/q_s) during the exponential fed-batch phase for each cultivation, which are 0.37, 0.22 and 0.16 for the 5 min pulse, 10 min pulse, and the reference cultivation, respectively.

The acetate cycling fluxes (Figure 3d–f) show a higher specific acetate reassimilation rate for the reference cultivation. Therefore, although there was some amount of acetate produced in these cultivations, the higher reassimilation rate did not allow acetate accumulation in the medium. According to the acetate cycling concept (Anane et al., 2017), the difference in acetate reassimilation rates, relative to its production

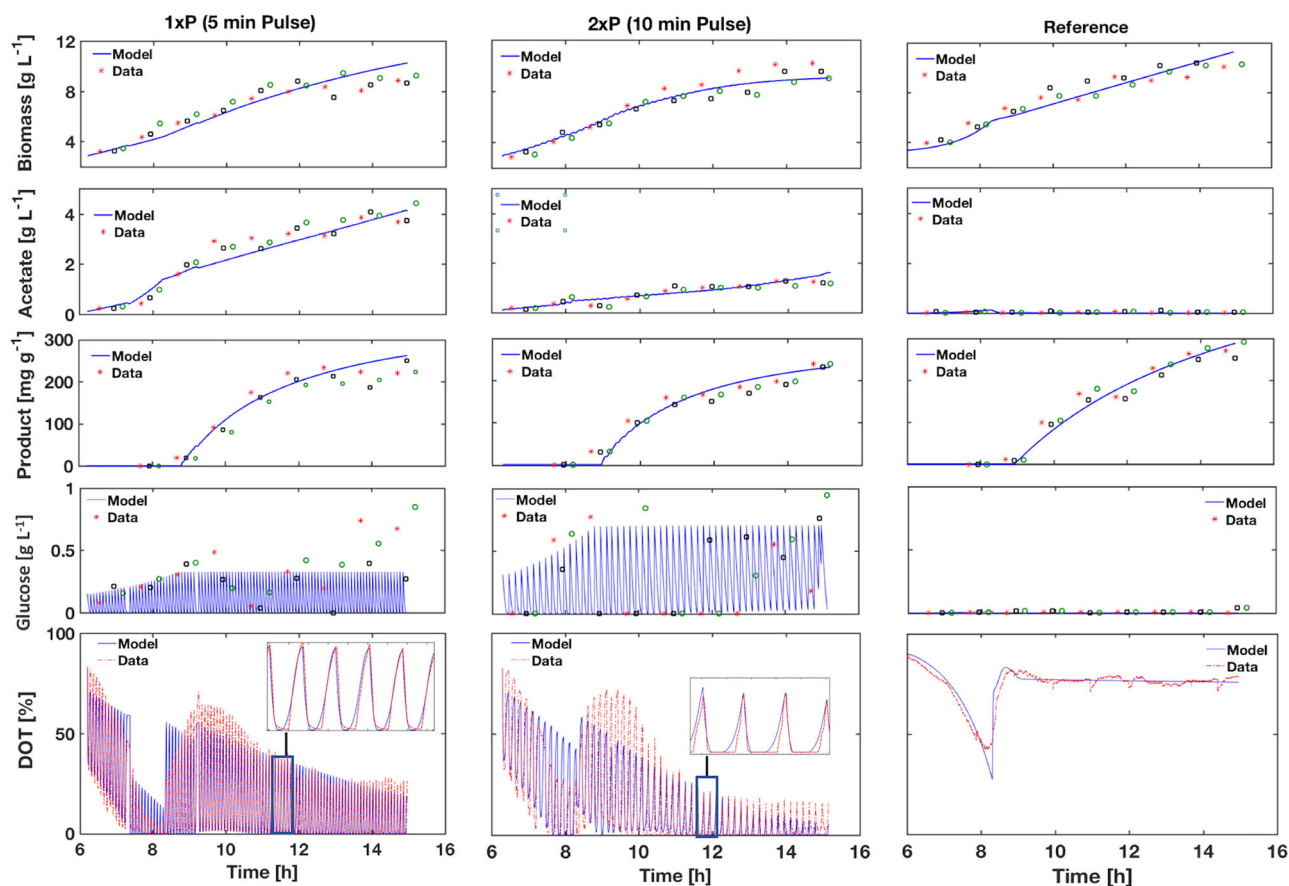


FIGURE 2 Fitting of a mechanistic model to data of pulse-based scale-down cultivations in the mini-bioreactors. All the data points of the triplicate run for three selected conditions (5 min pulses with 0.5 mM IPTG, 10 min pulses with 0.5 mM IPTG, and the reference) were pooled together for the parameter estimation (except for DOT). Cultivations are shown from the start of the feeding phase at 6 hr. Induction with IPTG was performed at 9 hr. IPTG, isopropyl- β -D-thiogalactopyranosid. Symbols: \square , $*$, and \odot are triplicate runs—model [Color figure can be viewed at wileyonlinelibrary.com]

rates, is what actually leads to different acetate concentrations in the extracellular medium in the cultivations.

In addition, the specific growth rates that were achieved in the exponential feed fed-batch phase were higher than the setpoint ($\mu_{\text{set}} = 0.35 \text{ hr}^{-1}$) in the pulse-based cultivations (13% higher for 5 min, 33% higher for 10 min). The deviation from the set point of the specific growth rate seemed to be directly proportional to the magnitude of the glucose pulses (Figure 3g). Probably due to higher maintenance energy (Table 2) in the pulse-based cultivations, there was a higher oxygen consumption rate in these bioreactors (Figure 3h) than in the reference cultivation, whereas the specific product formation rate was higher in the reference cultivation than in the pulse-based cultivations (Figure 3i).

3.4 | Accumulation and incorporation of noncanonical amino acids into proinsulin

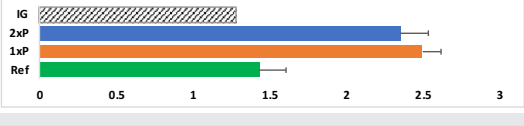
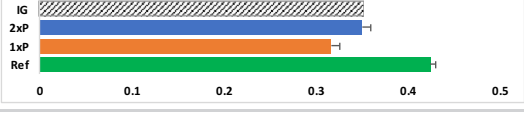
Generally, there was a higher concentration of norvaline in the intracellular soluble fraction than in the purified inclusion bodies for

all cultivation conditions. For instance, in the 5 and 10 min glucose pulse cultivations (without background glucose feeding), there were, respectively, five and three times higher norvaline in the intracellular soluble fraction than in the purified inclusion bodies (Figure 4a). Because the recombinant protein used for this study is very rich in leucine with only a few methionine and isoleucine residues (Reitz et al., 2018), much of the discussion is based on the exchange of leucine for norvaline in the product, while the plots showing the incorporation of the noncanonical amino acids norleucine and β -methyl-norleucine are given in the Supporting Information Material.

The norvaline to leucine ratio in the inclusion bodies from the 5 min pulse cultivations was approximately 50 times higher than in the reference cultivation, whereas the 10 min pulse cultivations had approximately 30 times higher norvaline incorporation levels (norvaline-leucine ratio) compared with the reference cultivation (Figure 4b).

The frequency of the pulses also affected the kinetics of norvaline incorporation (Figure 4c). At higher pulse frequencies, there was a more rapid incorporation rate, which seemed to

TABLE 2 Results of parameter estimation for scale-down fed-batch cultivation in miniaturized bioreactors, showing the maximum specific rates and yield coefficients of *E. coli* in response to the induced glucose pulses

Parameter	Estimated values	Notes
q_{Smax} ($g \cdot g^{-1} \cdot hr^{-1}$)		In agreement with the results of Lin, Mathiszik, Xu, Enfors, and Neubauer (2001) and Brand, Junne, Anane, Cruz-Bournazou, and Neubauer (2018), the <i>E. coli</i> strain developed a higher capacity for glucose uptake in the presence of glucose pulses, where the adaptation of the maximum uptake capacity seems to be proportional to the pulse size
K_s ($g \cdot L^{-1}$)		Both pulse-based cultivations resulted in higher K_s values than the reference cultivation, which implies that the <i>E. coli</i> strain developed a lower affinity for glucose under the induced concentration gradients
q_{pAmax} ($g \cdot g^{-1} \cdot hr^{-1}$)		Interesting to note that the specific maximum acetate production rate is the same in both the 5 min pulse-based and reference cultivations. The difference in acetate profiles must, therefore, be accounted for by other parameters such as differences in its reassimilation rates
q_{Amax} ($g \cdot g^{-1} \cdot hr^{-1}$)		Under homogeneous conditions, there is a higher acetate reassimilation rate, which results in lower extracellular acetate than under pulse-based conditions. Within the pulses, the reassimilation rate of acetate in the 5 min pulses is slightly lower than in 10 min pulses which is reflected in the acetate profiles
q_m ($g \cdot g^{-1} \cdot hr^{-1}$)		Homogeneous cultivation conditions led to lower maintenance energy. Higher frequency glucose pulses divert more energy towards maintenance than low-frequency pulses
Y_{Oa} ($g \cdot g^{-1}$)		Both pulse-based cultivations used up more oxygen for oxidation of acetate than in the reference. This yield coefficient is directly linked to the specific oxygen uptake rate (qO) in the model
Y_{Os} ($g \cdot g^{-1}$)		Oxygen requirements for glucose oxidation in the pulse-based cultivation were higher than in reference. This may be linked to the higher maintenance energy requirements under heterogeneous cultivation conditions
Y_{xs} ($g \cdot g^{-1}$)		Without taking maintenance energy into consideration and biomass gained from acetate consumption, there seemed to be a higher yield of biomass on glucose in the pulse-based cultivation than in the reference cultivations
Y_{px} ($g \cdot g^{-1}$)		In terms of recombinant product yield, the pulses had a negative effect on product formation. The reference cultivation had the highest mass of inclusion bodies of proinsulin per gram of biomass

Note: Error bars represent the standard deviation for each parameter estimate, which was calculated using the method of covariance matrix based on sensitivity matrix, as described by López C, Wozny, Flores-Tlacuahuac, Vasquez-Medrano, and Zavala (2016).

Abbreviations: 1xP, 5 min glucose pulse cultivation; 2xP, 10 min glucose pulse cultivation; IG, initial guesses (also used to calculate the feed profiles); Ref, reference cultivation.

reach saturation levels approximately 4 hr after protein induction. Conversely, the low-frequency pulses led to a more gradual incorporation rate at the beginning, but this seemed not to reach any saturation levels for all the 6 hr that were investigated after induction.

The presence of glucose in the background of the pulses lowered the concentration of norvaline in both the recombinant product and

cellular material (Figure 4b). For the same cultivation conditions (e.g., 5 min pulse, 0.5 mM IPTG), the runs that had background enzymatic glucose release had a 10 times lower norvaline incorporation than the cultivations without the background glucose feed. Thus, in situations where the cells were prevented from experiencing acute glucose starvation, the level of incorporation was less than when complete glucose depletion occurred between pulses.

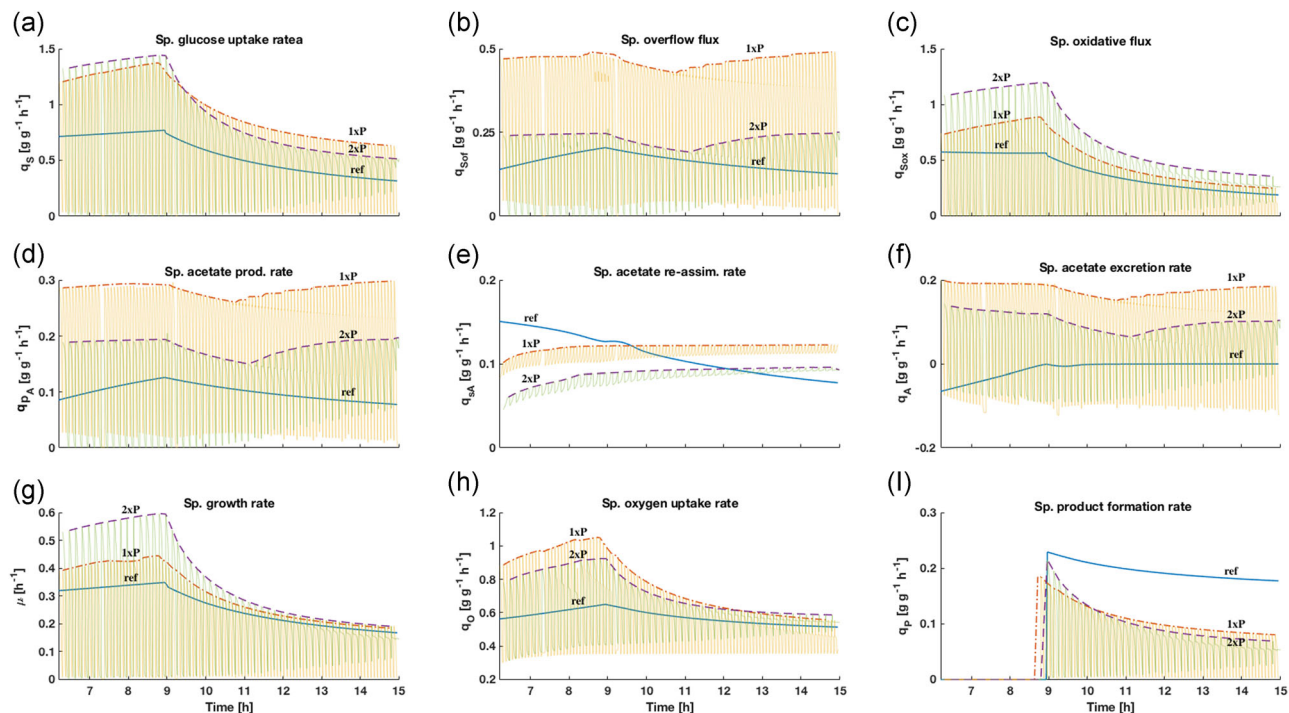


FIGURE 3 Profiles of metabolic fluxes of *E. coli* BW25113 pSW3 during the different cultivation conditions. The other two are fed-batch cultivations with a pulse-based feed of glucose every 5 min (1xP) and every 10 min (2xP). Both of these pulse-based cultivations were induced to 0.5 mM IPTG with no glucose supply in the background. The broken lines depict the overall trend of the fluxes, whereas the actual data of the pulse-based cultivations are shown as the oscillations in the background. Note that negative secretion rates are shown when acetate is consumed. Cultivations are shown from the start of the feeding phase at 6 hr, with induction at 9 hr. IPTG, isopropyl- β -D-thiogalactopyranosid; ref, reference cultivation with smooth glucose supply; sp, specific [Color figure can be viewed at wileyonlinelibrary.com]

4 | DISCUSSION

We report the development of a high-throughput mini-bioreactor scale-down platform for investigating the effects of heterogeneous cultivation conditions, particularly glucose and dissolved oxygen gradients on *E. coli* fed-batch cultivation, at the early bioprocess development phase. As opposed to strain screening and fermentation

development under homogeneous cultivation conditions, the results of the scale-down cultivations in the current study show significant variations in strain behavior in response to different cultivation conditions. In particular, the cultivations that were subjected to pure glucose pulses with accompanying limitation in dissolved oxygen supply (Figure 2) showed higher extracellular metabolite concentrations, low biomass, low product yields, and overall poor performance

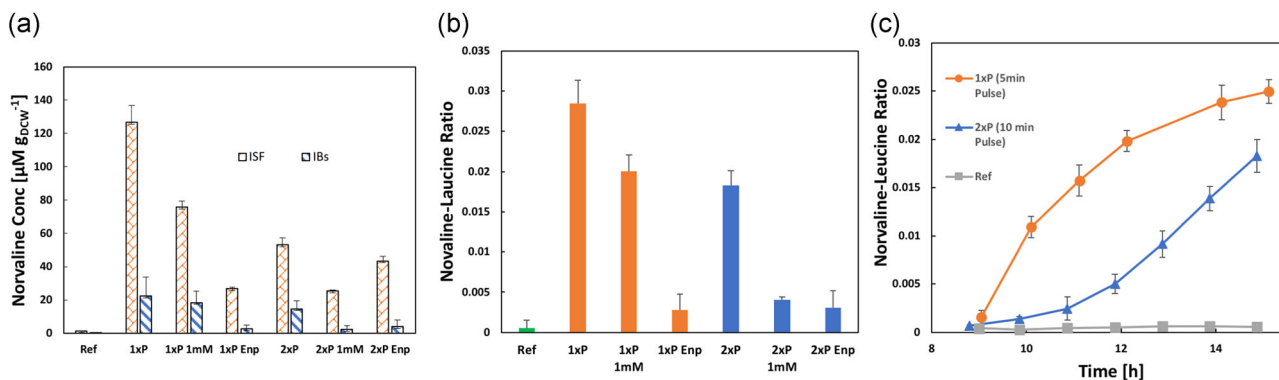


FIGURE 4 Influence of glucose pulses on the concentration of the noncanonical amino acid norvaline. (a) Intracellular soluble fraction and purified inclusion bodies (IBs); (b) incorporation levels in the purified inclusion bodies for all the cultivation conditions presented in Table 1; (c) dynamic profile of norvaline incorporation (both 0.5 mM IPTG) as a function of glucose pulse frequency (1xP and 2xP). 1xP, 5 min glucose pulse cultivation; 2xP, 10 min glucose pulse cultivation; Enp, cultivation with enzymatic glucose release; IPTG, isopropyl- β -D-thiogalactopyranosid; Ref, reference cultivation [Color figure can be viewed at wileyonlinelibrary.com]

compared with the reference cultivations. The results obtained in the 10 ml mini-bioreactor scale-down cultivations are similar to the results of previous scale-down studies in bench-top bioreactors (1–20 L), in terms of higher extracellular metabolite concentrations under high-frequency stresses (Neubauer, Haggström, & Enfors, 1995), higher metabolic fluxes under stressful conditions (Sunya, Bideaux, Molina-Jouve, & Gorret, 2013) and accumulation of norvaline under oxygen perturbations (Soini, Ukkonen, & Neubauer, 2011). The application of the mechanistic model in this study was central to the development of the scale-down framework in two ways: (a) The use of the model to calculate the gradient profiles in the experiments and (b) the use of the model to evaluate the results, which are further discussed in the following sections.

4.1 | Model-based design of scale-down cultivations

The incorporation of the mechanistic model to the robotic LHS to execute calculated set-points was an important step in the mini-bioreactor scale-down cultivations. As pointed out by Tajsoleiman et al. (2019), the configuration of miniaturized bioreactors to achieve real gradient profiles for scale-down studies is challenging. Therefore, in this study, we leveraged on the capability of mechanistic modeling and LHS to achieve approximate gradients that resulted in physiological responses similar to those observed in large-scale bioreactors while keeping a high degree of automation and parallelization. The initial parameters of the model were obtained from prior cultivations (e.g., see Anane, Sawatzki et al., 2019) and shown in Table 2. We used a macrokinetic model to compare the dynamical differences in formation and inhibition kinetics under the experimental cultivation conditions. Differences in growth capacities, robustness and product formation could be inferred from the deviation of the parameter estimates after fitting the model to the experimental data (Figure 3). The use of a single set of model parameters for pulse-size calculation for all cultivations helps to establish a baseline, which allows the comparison of parallel cultivations. The model calculations and robotic executions also helped to establish and trace cause-and-effect relationships between process conditions and physiological responses, which are important for the interpretation of the results. Although a fully integrated genome-scale model of the strain (Weaver, Keseler, Mackie, Paulsen, & Karp, 2014) coupled with a hydrodynamic model of the larger scale (Haringa et al., 2018) may give more accurate results, the simplified mechanistic model used here was adequate for the purpose of calculating the concentration gradients, without the constraints of higher computational burden and issues of parameter identifiability in larger models, as discussed by Anane et al. (2019). The further development of the system to simultaneously carry out 21 parallel cultivations ensured the generation of a large amount of data within the shortest possible time and eliminated batch-to-batch variability in inoculum and media components. Other process benefits, such

as higher reproducibility and reduced human interference, were also realized in the cultivations, due to the automated routines.

4.2 | Model-based evaluation of the scale-down cultivations

The metabolic adaptation of the strain to the various conditions over the period of the cultivation could be deduced from the mechanistic model fitting, as given by the maximum achievable specific rates under each cultivation condition in Table 2. The *E. coli* BW25113 psW3 strain showed a significant shift in these rates from efficient utilization of glucose (low ratios of \bar{q}_{sof} to \bar{q}_s) under homogeneous cultivation conditions to carbon wasting through overflow routes (high ratios of \bar{q}_{sof} to \bar{q}_s) under the pulse-based cultivations. This shift in metabolic states is further seen in the higher values of the parameters q_{Amax} and q_{pAmax} in the pulse-based cultivations compared with the reference cultivation (Table 2). The model fitting further showed strong parameter dependencies on specific cultivation conditions. For instance, variations in the values of the affinity constant K_s in relation to the residual glucose under each cultivation condition determines the sensitivity of the strain to the heterogeneous environment. Our results provide the experimental evidence to support this thesis as previously reported by Haringa, Deshmukh, Mudde, and Noorman (2017). The model fitting revealed an increasing K_s value with increasing pulse frequency, which means that under the higher gradient conditions, the cells were adapting to a different metabolic regime that would make them less sensitive to the heterogeneous environment.

In addition, the glucose pulses led to a significant deviation of the specific growth rates from the set-points in the exponential feed fed-batch phase, as deduced from the model fitting. In the presence of low frequency gradients, which are usually present in large industrial bioreactors (Lara, Galindo, Ramírez, & Palomares, 2006), the cells are occasionally exposed to substrate concentration pockets that may trigger growth at μ_{max} , although they are still in fed-batch phase where growth is supposed to be controlled well below μ_{max} . This loss of physiological control, as observed in this study, may contribute to the lack of process reproducibility in industrial-scale cultivations.

Another important aspect of the metabolic response to the heterogeneous cultivation conditions is that *E. coli* tends to maintain higher metabolic fluxes in the presence of gradients (Figure 3), which in some cases can lead to higher viability in heterogeneous environments than in homogenous environments (Sunya et al., 2013). However, as shown in the product profiles (Figure 2), this higher viability does not necessarily translate into higher productivity in recombinant protein processes. Rather, the higher metabolic states may channel energy towards maintenance and adaptation of the strain to the heterogeneous environment, as seen in the profiles of the specific oxygen uptake rates under the various conditions (Table 2).

The scale-down condition with the background enzymatic glucose feed represents the situation in the large-scale bioreactor where the cells are occasionally exposed to excess glucose

conditions, but not acute starvation zones. This zone may be in the vicinity of recirculation loops in broths that are mixed by Rushton turbine impellers on the large scale. This scale-down condition led to relatively lower extracellular metabolite concentrations, slightly higher biomass concentrations, and a lower concentration of ncBCAAs. The continuous supply of background glucose by the enzymatic feeding system may maintain substrate concentrations close to the K_s value of the organism. This ensures that a steady pool of intracellular metabolites is maintained in the cell, which prevents the starvation responses that were apparent in the pure pulse feed conditions.

4.3 | Recombinant product quantity and quality considerations

From the results (Figure 3i), it is apparent that the specific product formation rate was lower in the pulse-based cultivations compared with the reference cultivation. Apart from the previously discussed metabolic effects (high overflow conditions), varying plasmid copy numbers in response to the heterogeneous conditions could also contribute to the lower product formation rate in the presence of oscillations in glucose and oxygen concentrations (Smith & Bidochka, 1998), although the plasmid copy number per cell was not analyzed. As observed for the concentration of extracellular metabolites, the higher frequency pulses have a clear influence on the product quality (incorporation of ncBCAAs) more adversely than the low-frequency gradients (Figure 4b). We observed a close relationship between the profiles of extracellular metabolites and the accumulation of norvaline in the cells, possibly due to the ability of the leucine synthesis genes to use the accumulated pyruvate as a substrate to synthesize α -keto-butyrate and further α -keto-valerate (Soini et al., 2011), which are precursors for the production of the ncBCAAs. The higher concentrations of these ncBCAAs in the intracellular soluble fraction than in the inclusion bodies (Figure 4a) confirm the hypothesis that they first accumulate in the cellular material under stressful cultivation conditions. Then, as their concentrations increase, there is an increased probability of misacylation of transfer RNA molecules with the ncBCAAs, due to the similarity in structure to their canonical isoforms (Jones, Alexander, & Pan, 2011; Reitz et al., 2018). The cultures that were induced to a higher inducer concentration had a lower level of incorporation of norvaline than those with lower IPTG concentration (Figure 4b). This observation is interesting because it shows that apart from the heterogeneous conditions, the induction strength can also influence the quality of the recombinant product.

5 | CONCLUSIONS

Bioprocess development is very time consuming and labor-intensive, requiring several experimental runs to characterize a bioproduct and its production process. The development of high-throughput robotic cultivation platforms is a promising technology, which facilitates both strain screening and fermentation process development. Nevertheless, as the complexity of the cultivation strategy increases, model-based tools

are required to design and operate the robotic facilities. The use of the mechanistic model (which is derived from the physiology of the strain) to define the gradient profiles for the various scale-down conditions is key to achieving real stress responses that are significant for evaluating the efficiency of *E. coli* bioprocesses. We prove that the specific perturbation conditions have a direct impact on many of the model parameters that describe the cell physiology. This indicates that the use of an appropriate scale-down model is important for the development of large-scale models that include the cell physiology. Furthermore, model-based identification of the cellular parameters provides an important tool for the selection of strains in the screening phase, which exhibit improved performance under large-scale conditions. This would help to select the most robust strains for further development and subsequent bioprocess scale-up.

ACKNOWLEDGMENTS

We dedicate this paper to the late Hong Ying Lin whose work on pulsed feeding was an important motivation for this project. We are grateful for financial support from the European Union's Horizon 2020 research and innovation program under the Marie Skłodowska-Curie actions grant agreement No. 643056 (Biorapid). We would also like to thank Dr. Sebastian Riedel and Dr. Florian Glauche for their support with experimental equipment. Additionally, we thank Roche Diagnostics International Ltd. for the supply of the Cedex Bio HT analyser.

CONFLICT OF INTERESTS

The authors declare that there are no conflict of interests.

SUPPLEMENTARY DATA

The MATLAB® codes and fermentation data can be found at https://gitlab.tubit.tu-berlin.de/nicolas.cruz/E_coli_fed_batch/tree/master/Anane_2019c_B&B

ORCID

Emmanuel Anane  <http://orcid.org/0000-0001-8143-7551>

Benjamin Haby  <http://orcid.org/0000-0002-7417-5175>

Sebastian Hans  <http://orcid.org/0000-0002-5346-869X>

Niels Krausch  <http://orcid.org/0000-0003-2325-6001>

Mariano Nicolas Cruz Bournazou  <http://orcid.org/0000-0001-9461-4414>

REFERENCES

- Anane, E., López C, D. C., Barz, T., Sin, G., Gernaey, K. V., Neubauer, P., & Cruz Bournazou, M. N. (2019). Output uncertainty of dynamic growth models: Effect of uncertain parameter estimates on model reliability. *Biochemical Engineering Journal*, 150, 107247. <https://doi.org/10.1016/j.bej.2019.107247>

- Anane, E., López C, D. C., Neubauer, P., & Cruz Bournazou, M. N. (2017). Modelling overflow metabolism in *Escherichia coli* by acetate cycling. *Biochemical Engineering Journal*, 125, 23–30. <https://doi.org/10.1016/j.bej.2017.05.013>
- Anane, E., Sawatzki, A., Neubauer, P., & Cruz-Bournazou, M. N. (2019). Modelling concentration gradients in fed-batch cultivations of *E. coli* - towards the flexible design of scale-down experiments. *Journal of Chemical Technology & Biotechnology*, 94(2), 516–526. <https://doi.org/10.1002/jctb.5798>
- Back, A., Rossignol, T., Krier, F., Nicaud, J. -M., & Dhulster, P. (2016). High-throughput fermentation screening for the yeast *Yarrowia lipolytica* with real-time monitoring of biomass and lipid production. *Microbial Cell Factories*, 15(1), 147. <https://doi.org/10.1186/s12934-016-0546-z>
- Barz, T., Sommer, A., Wilms, T., Neubauer, P., & Cruz Bournazou, M. N. (2018). Adaptive optimal operation of a parallel robotic liquid handling station. *IFAC-PapersOnLine*, 51(2), 765–770. <https://doi.org/10.1016/j.ifacol.2018.04.006>
- Brand, E., Junne, S., Anane, E., Cruz-Bournazou, M. N., & Neubauer, P. (2018). Importance of the cultivation history for the response of *Escherichia coli* to oscillations in scale-down experiments. *Bioprocess and Biosystems Engineering*, 41, 1305. <https://doi.org/10.1007/s00449-018-1958-4>
- Bylund, F., Castan, A., Mikkola, R., Veide, A., & Larsson, G. (2000). Influence of scale-up on the quality of recombinant human growth hormone. *Biotechnology and Bioengineering*, 69(2), 119–128. [https://doi.org/10.1002/\(SICI\)1097-0290\(20000720\)69:2<119::AID-BIT1>3.0.CO;2-9](https://doi.org/10.1002/(SICI)1097-0290(20000720)69:2<119::AID-BIT1>3.0.CO;2-9)
- Cruz Bournazou, M. N., Barz, T., Nickel, D. B., Lopez Cárdenas, D. C., Glauche, F., Knepper, A., & Neubauer, P. (2017). Online optimal experimental re-design in robotic parallel fed-batch cultivation facilities. *Biotechnology and Bioengineering*, 114(3), 610–619. <https://doi.org/10.1002/bit.26192>
- Enfors, S. O., Jahic, M., Rozkov, A., Xu, B., Hecker, M., Jürgen, B., ... Manelius, A. (2001). Physiological responses to mixing in large scale bioreactors. *Journal of Biotechnology*, 85(2), 175–185.
- Gebhardt, G., Hortsch, R., Kaufmann, K., Arnold, M., & Weuster-Botz, D. (2011). A new microfluidic concept for parallel operated milliliter-scale stirred tank bioreactors. *Biotechnology Progress*, 27(3), 684–690. <https://doi.org/10.1002/btpr.570>
- Glazyrina, J., Materne, E. -M., Dreher, T., Storm, D., Junne, S., Adams, T., ... Neubauer, P. (2010). High cell density cultivation and recombinant protein production with *Escherichia coli* in a rocking-motion-type bioreactor. *Microbial Cell Factories*, 9(1), 42. <https://doi.org/10.1186/1475-2859-9-42>
- Grenier, F., Matteau, D., Baby, V., & Rodrigue, S. (2014). Complete genome sequence of *Escherichia coli* BW25113. *Genome Announcements*, 2(5), 90005. <https://doi.org/10.1128/genomeA.01038-14>
- Haringa, C., Deshmukh, A. T., Mudde, R. F., & Noorman, H. J. (2017). Euler-Lagrange analysis towards representative down-scaling of a 22 m³ aerobic *S. cerevisiae* fermentation. *Chemical Engineering Science*, 170, 653–669. <https://doi.org/10.1016/j.ces.2017.01.014>
- Haringa, C., Tang, W., Wang, G., Deshmukh, A. T., van Winden, W. A., Chu, J., ... Noorman, H. J. (2018). Computational fluid dynamics simulation of an industrial *P. chrysogenum* fermentation with a coupled 9-pool metabolic model: Towards rational scale-down and design optimization. *Chemical Engineering Science*, 175, 12–24. <https://doi.org/10.1016/j.ces.2017.09.020>
- Hemmerich, J., Noack, S., Wiechert, W., & Oldiges, M. (2018). Microbioreactor systems for accelerated bioprocess development. *Biotechnology Journal*, 13(4), 1–9. <https://doi.org/10.1002/biot.201700141>
- Janakiraman, V., Kwiatkowski, C., Kshirsagar, R., Ryll, T., & Huang, Y. -M. (2015). Application of high-throughput mini-bioreactor system for systematic scale-down modeling, process characterization, and control strategy development. *Biotechnology Progress*, 31(6), 1623–1632. <https://doi.org/10.1002/btpr.2162>
- Jones, T. E., Alexander, R. W., & Pan, T. (2011). Misacylation of specific nonmethionyl tRNAs by a bacterial methionyl-tRNA synthetase. *Proceedings of the National Academy of Sciences*, 108(17), 6933–6938. <https://doi.org/10.1073/pnas.1019033108>
- Krause, M., Neubauer, A., & Neubauer, P. (2016). The fed-batch principle for the molecular biology lab: Controlled nutrient diets in ready-made media improve production of recombinant proteins in *Escherichia coli*. *Microbial Cell Factories*, 15(1), 1–13. <https://doi.org/10.1186/s12934-016-0513-8>
- Krause, M., Ukkonen, K., Haataja, T., Ruottinen, M., Glumoff, T., Neubauer, A., ... Vasala, A. (2010). A novel fed-batch based cultivation method provides high cell-density and improves yield of soluble recombinant proteins in shaken cultures. *Microbial Cell Factories*, 9, 11. <https://doi.org/10.1186/1475-2859-9-11>
- Lara, A. R., Galindo, E., Ramírez, O. T., & Palomares, L. A. (2006). Living with heterogeneities in bioreactors: Understanding the effects of environmental gradients on cells. *Molecular Biotechnology*, 34(3), 355–382. <https://doi.org/10.1385/MB:34:3:355>
- Lin, H. Y., Mathisizik, B., Xu, B., Enfors, S. O., & Neubauer, P. (2001). Determination of the maximum specific uptake capacities for glucose and oxygen in glucose-limited fed-batch cultivations of *Escherichia coli*. *Biotechnology and Bioengineering*, 73(5), 347–357.
- López C, D. C., Wozny, G., Flores-Tlacuahuac, A., Vasquez-Medrano, R., & Zavala, V. M. (2016). A computational framework for identifiability and ill-conditioning analysis of lithium-ion battery models. *Industrial & Engineering Chemistry Research*, 55(11), 3026–3042.
- Mayer, S., Junne, S., Ukkonen, K., Glazyrina, J., Glauche, F., Neubauer, P., & Vasala, A. (2014). Lactose autoinduction with enzymatic glucose release: Characterization of the cultivation system in bioreactor. *Protein Expression and Purification*, 94, 67–72. <https://doi.org/10.1016/j.pep.2013.10.024>
- Neubauer, P., Häggström, L., & Enfors, S. -O. -O. (1995). Influence of substrate oscillations on acetate formation and growth yield in *Escherichia coli* glucose limited fed-batch cultivations. *Biotechnology and Bioengineering*, 47(2), 139–146. <https://doi.org/10.1002/bit.260470204>
- Neubauer, P., & Junne, S. (2010). Scale-down simulators for metabolic analysis of large-scale bioprocesses. *Current Opinion in Biotechnology*, 21(1), 114–121. <https://doi.org/10.1016/j.copbio.2010.02.001>
- Neubauer, P., & Junne, S. (2016). Scale-up and scale-down methodologies for bioreactors. In C. -F. Mandenius (Ed.), *Bioreactors: Design, operation and novel applications* (pp. 323–354). Weinheim, Germany: Wiley-VCH Verlag GmbH. <https://doi.org/10.1002/9783527683369.ch11>
- Nickel, D. B., Cruz-Bournazou, M. N., Wilms, T., Neubauer, P., & Knepper, A. (2017). Online bioprocess data generation, analysis, and optimization for parallel fed-batch fermentations in milliliter scale. *Engineering in Life Sciences*, 17(11), 1195–1201. <https://doi.org/10.1002/elsc.201600035>
- Nienow, A. W., Scott, W. H., Hewitt, C. J., Thomas, C. R., Lewis, G., Amanullah, A., ... Meier, S. J. (2013). Scale-down studies for assessing the impact of different stress parameters on growth and product quality during animal cell culture. *Chemical Engineering Research and Design*, 91(11), 2265–2274. <https://doi.org/10.1016/j.cherd.2013.04.002>
- Panula-Perälä, J., Siurkus, J., Vasala, A., Wilmanowski, R., Casteleijn, M. G., & Neubauer, P. (2008). Enzyme controlled glucose auto-delivery for high cell density cultivations in microplates and shake flasks. *Microbial Cell Factories*, 12, 31. <https://doi.org/10.1186/1475-2859-7-31>
- Philip, P., Kern, D., Goldmanns, J., Seiler, F., Schulte, A., Habicher, T., & Büchs, J. (2018). Parallel substrate supply and pH stabilization for optimal screening of *E. coli* with the membrane-based fed-batch shake flask. *Microbial Cell Factories*, 17(1), 69. <https://doi.org/10.1186/s12934-018-0917-8>

- Puskeiler, R., Kaufmann, K., & Weuster-Botz, D. (2005). Development, parallelization, and automation of a gas-inducing milliliter-scale bioreactor for high-throughput bioprocess design (HTBD). *Biotechnology and Bioengineering*, 89(5), 512–523. <https://doi.org/10.1002/bit.20352>
- Reitz, C., Fan, Q., & Neubauer, P. (2018). Synthesis of non-canonical branched-chain amino acids in *Escherichia coli* and approaches to avoid their incorporation into recombinant proteins. *Current Opinion in Biotechnology*, 53, 248–253. <https://doi.org/10.1016/j.copbio.2018.05.003>
- Sawatzki, A., Hans, S., Narayanan, H., Haby, B., Krausch, N., Sokolov, M., ... Cruz Bournazou, M. (2018). Accelerated bioprocess development of endopolygalacturonase-production with *Saccharomyces cerevisiae* using multivariate prediction in a 48 mini-bioreactor automated platform. *Bioengineering*, 5(4), 101. <https://doi.org/10.3390/bioengineering5040101>
- Smith, M. A., & Bidochka, M. J. (1998). Bacterial fitness and plasmid loss: The importance of culture conditions and plasmid size. *Canadian Journal of Microbiology*, 44(4), 351–355.
- Soini, J., Ukkonen, K., & Neubauer, P. (2011). Accumulation of amino acids deriving from pyruvate in *Escherichia coli* W3110 during fed-batch cultivation in a two-compartment scale-down bioreactor. *Advances in Bioscience and Biotechnology*, 02(05), 336–339. <https://doi.org/10.4236/abb.2011.25049>
- Sunya, S., Bideaux, C., Molina-Jouve, C., & Gorret, N. (2013). Short-term dynamic behavior of *Escherichia coli* in response to successive glucose pulses on glucose-limited chemostat cultures. *Journal of Biotechnology*, 164(4), 531–542. <https://doi.org/10.1016/j.jbiotec.2013.01.014>
- Tajsoleiman, T., Mears, L., Krühne, U., Gernaey, K. V., & Cornelissen, S. (2019). An industrial perspective on scale-down challenges using miniaturized bioreactors. *Trends in Biotechnology*, 0(0), 1–10. <https://doi.org/10.1016/j.tibtech.2019.01.002>
- Velez-Suberbie, M. L., Betts, J. P. J., Walker, K. L., Robinson, C., Zoro, B., & Keshavarz-Moore, E. (2018). High throughput automated microbial bioreactor system used for clone selection and rapid scale-down process optimization. *Biotechnology Progress*, 34(1), 58–68. <https://doi.org/10.1002/btpr.2534>
- Vester, A., Hans, M., Hohmann, H. P., & Weuster-Botz, D. (2009). Discrimination of riboflavin producing *Bacillus subtilis* strains based on their fed-batch process performances on a millilitre scale. *Applied Microbiology and Biotechnology*, 84(1), 71–76. <https://doi.org/10.1007/s00253-009-1966-z>
- Weaver, D. S., Keseler, I. M., Mackie, A., Paulsen, I. T., & Karp, P. D. (2014). A genome-scale metabolic flux model of *Escherichia coli* K-12 derived from the EcoCyc database. *BMC Systems Biology*, 8(1), 1–24. <https://doi.org/10.1186/1752-0509-8-79>

SUPPORTING INFORMATION

Additional supporting information may be found online in the Supporting Information section.

How to cite this article: Anane E, García AC, Haby B, et al. A model-based framework for parallel scale-down fed-batch cultivations in mini-bioreactors for accelerated phenotyping. *Biotechnology and Bioengineering*. 2019;116:2906–2918. <https://doi.org/10.1002/bit.27116>